


Article

Probabilistic Assessment of the Dynamic Viscosity of Self-Compacting Steel-Fiber Reinforced Concrete through a Micromechanical Model

Ángel De La Rosa ^{1,*}, Gonzalo Ruiz ¹, Enrique Castillo ² and Rodrigo Moreno ³

¹ ETS de Ingenieros de Caminos, C. y P., Universidad de Castilla-La Mancha, Av. Camilo José Cela s/n, 13071 Ciudad Real, Spain; gonzalo.ruiz@uclm.es

² Real Academia de Ingeniería, Don Pedro 10, 28005 Madrid, Spain; castie@unican.es

³ Instituto de Cerámica y Vidrio (CSIC), C. Kelsen 5, Campus de Cantoblanco, 28049 Madrid, Spain; rmoreno@icv.csic.es

* Correspondence: angel.delarosa@uclm.es

Abstract: This article develops a probabilistic approach to a micromechanical model to calculate the dynamic viscosity in self-compacting steel-fiber reinforced concrete (SCSFRC), which implies a paradigm shift in the approach of the deterministic models used. It builds on a previous work by the authors in which Bayesian analysis is applied to rheological micromechanical models in cement paste, self-compacting mortar, and self-compacting concrete. As a consequence of the varied characteristics of the particles in these suspensions (in terms of materials, shapes, size distributions, etc.), as well as their random nature, it seems appropriate to study these systems with probabilistic models. The Bayesian analysis, thorough Markov Chain Monte Carlo and Gibbs Sampling methods, allows the conversion of parametric-deterministic models into parametric-probabilistic models, which results in enrichment in engineering and science. The incorporation of steel fibers requires a new term in the model to account for their effect on the dynamic viscosity of SCSFRC, and this new term is also treated here with the Bayesian approach. The paper uses an extensive collection of experimental data to obtain the probability density functions of the parameters for assessing the dynamic viscosity in SCSFRC. The results obtained with these parameters' distributions are much better than those calculated with the theoretical values of the parameters, which indicates that Bayesian methods are appropriated to respond to questions in complex systems with complex models.

Keywords: self-compacting steel-fiber reinforced concrete; dynamic viscosity; micromechanical constitutive model; deterministic and probabilistic models; Bayesian analysis



Citation: De La Rosa, Á.; Ruiz, G.; Castillo, E.; Moreno, R. Probabilistic Assessment of the Dynamic Viscosity of Self-Compacting Steel-Fiber Reinforced Concrete through a Micromechanical Model. *Materials* **2022**, *15*, 2763. <https://doi.org/10.3390/ma15082763>

Academic Editors: Costantino Menna and Lizhi Sun

Received: 4 February 2022

Accepted: 7 April 2022

Published: 9 April 2022

Publisher's Note: MDPI stays neutral with regard to jurisdictional claims in published maps and institutional affiliations.



Copyright: © 2022 by the authors. Licensee MDPI, Basel, Switzerland. This article is an open access article distributed under the terms and conditions of the Creative Commons Attribution (CC BY) license (<https://creativecommons.org/licenses/by/4.0/>).

1. Introduction

Understanding the rheological behavior of cementitious suspensions is essential for new technological applications of concrete [1,2], such as pumping processes or digital manufacturing [3–10], as well as to carry out specific numerical simulations [11–13]. Advanced methods for the design of high-performance concrete [14–17] require knowing the values of their main rheological parameters. Particularly, the dynamic viscosity of this type of cementitious suspensions can be calculated from the experimental flow curve (shear stress–shear rate) using a Bingham-type linear fit model or estimated with the Krieger and Dougherty analytical equation [18] which correctly adjusts experimental rheological measurements carried out on cement pastes [19,20]. Besides, this analytical model is the foundation of advanced design methodologies for self-compacting concrete [14] and self-compacting steel-fiber reinforced concrete [15,17].

The Krieger and Dougherty equation, see Equation (1), consists of three parameters that have physical significance: The dynamic viscosity of the fluid phase, the maximum packing fraction, and the intrinsic viscosity of the particles (disperse phase). The dynamic

viscosity of the fluid phase can be measured with greater or lower precision depending on the degree of complexity that it has in terms of being able to be considered in this phase, again, as a suspension [21]. The shape and the size distribution of the particles are the parameters on which the maximum packing fraction of the disperse solid phase, ϕ_m , depends [19,22,23]. The intrinsic viscosity, $[\eta]$, measures the individual effect of particles on viscosity [19,22]. It is a parameter closely related to the characteristics of the aggregates as well [24–26], i.e., the shape, the angularity, the roughness [27], and the circularity of the particles [24,26].

$$\frac{\eta}{\eta_0} = \left(1 - \frac{\phi}{\phi_m}\right)^{-[\eta] \phi_m} \quad (1)$$

where

η : Suspension's dynamic viscosity.

η_0 : Fluid phase's dynamic viscosity.

ϕ : Solid phase's volume fraction.

ϕ_m : Maximum packing fraction of particles.

$[\eta]$: Intrinsic viscosity of the system.

Self-compacting steel-fiber reinforced concrete (SCSFRC) is more complex than self-compacting concrete as a consequence of the inclusion of needle-shaped particles (steel fibers) which interact with granular and powder materials, giving rise to a more heterogeneous cementitious suspension. This polydisperse system of particles in suspension in a viscous homogeneous fluid phase makes it challenging to measure its rheological behaviour. Thus, it is necessary to use analytical or semi-empirical models that offer a good approximation of the rheological parameters of the suspension. If the Krieger and Dougherty equation allows estimating the dynamic viscosity of a cementitious suspension, such as cement paste or self-compacting mortar and concrete, other micromechanical models make it possible to predict the increase in dynamic viscosity produced by the addition of steel fiber into concrete [15,22,28,29].

The uncertainty associated with the variability of the rheological behavior in this type of cementitious suspension makes it interesting to convert this type of deterministic model to a model with random variables. We performed this Bayesian analysis of Equation (1) applied to cement paste, self-compacting mortar, and self-compacting concrete in a previous paper [21].

Bayesian statistics is an alternative to classical statistics since it allows defining the model parameters as random variables. In contrast, classical statistics would describe them with fixed values [30]. Bayesian statistics combine existing information about a problem and empirically observed data using probability guidelines, resulting in more reliable estimations and predictions [31]. Besides, Bayesian methodology allows obtaining large samples of the random variables (the parameters of the model) which can be considered as probability density functions instead of getting the point estimates of the parameters, which would be the object of classical statistics [30]. This fact supposes an enrichment of the models by offering unambiguous probabilistic information on the parameters of interest, which supposes a change of paradigm when proposing a model in engineering.

This article extends our work in [21] to SCSFRC, and its thesis consists in developing a methodology for the probabilistic assessment of the dynamic viscosity of SCSFRC through a micromechanical model. Thus, the purpose of the research is to apply a Bayesian methodology and enrich our model [15] by offering unambiguous probabilistic information on the parameters of interest. Moreover, we want to transform the cited deterministic model [15] into a probabilistic one with random variables. This topic falls at the core of rheology applied to SCSFRC, so it is of utmost importance for the technology of fiber concrete.

In this case, one more phase is added: Steel fibers. Based on the mix design methodology for SCSFRC developed by De La Rosa et al. [15], and with the experimental data obtained by Grünwald [32], a Bayesian analysis of the parameters of the constitutive

models for estimating the dynamic viscosity of the suspension is done. We use the Krieger and Dougherty equation [18], and the Ghanbari et al. model [22] with the simplification proposed in [15]. Their parameters are considered here as random variables with their probability density functions, and not as unique values within confidence intervals. To our knowledge, this is the first time that this way of defining the parameters of a micromechanical model of phase suspension applied to the rheology of the SCSFRC has been considered.

The structure of the article is as follows. Firstly, we explain the essentials of Bayesian analysis, and how it facilitates the conversion of a deterministic model into a probabilistic one. Next, the paper gives details about the procedure and methodology. The following section describes the experimental data and the results. Finally, we draw the main conclusions from the investigation.

2. Probabilistic and Bayesian Analysis of a Micromechanical Constitutive Model to Calculate the Dynamic Viscosity in SCSFRC

Probabilistic network models are extensively used in engineering [33]. A key to implementing them is the definition of multivariate random variables, for which the Bayesian analysis provides a unique tool as it guarantees the existence of multivariate density functions.

The parameters ϕ_m and $[\eta]$ of the equation of Krieger and Dougherty, Equation (1), which allows the prediction of the dynamic viscosity in cementitious suspensions, η , may be expressed in probabilistic terms as a consequence of the inherent random nature of the phenomenon. The same consequence can be drawn for the constitutive model of the fiber to be used. The idea arises from the fact that the parameters of Equation (1) can be treated as random variables, described by probability density functions, and not as a single value. Thus, the conversion of both models into probabilistic ones through the Bayesian analysis makes sense and is interesting for improving the assessment of the dynamic viscosity.

When we use frequentist statistics to calculate dynamic viscosity, it is considered a random variable of a parametric family. Thus, the problem is simplified to estimate the parameters of the equation. When Bayesian analysis is used, a set of parametric distribution families is taken into account, considering their parameters as random variables [34], thereby obtaining an extended family of mixtures that provides more freedom for the calculation process.

2.1. Sources of Randomness in Self-Compacting Steel-Fiber Reinforced Concrete

Self-compacting steel-fiber reinforced concrete may be understood as a system composed of several solid granular phases of one or various sizes (aggregates) with needle-shaped particles (steel fibers), all of them in a continuous phase, the cement paste [22]. The cement paste has an intrinsic random nature as a consequence of its colloidal behaviour and the interaction with superplasticizer molecules [34].

Aggregates are three-dimensional particles of different sizes, with irregular and random shapes, which influence the rheological properties of the cementitious suspensions of which they are a part. Their morphological characteristics are described by various geometric parameters related to dimensions, shape, angularity, surface roughness, etc. [35,36]. These parameters can be calculated through various techniques, such as digital image processing [37] or photogrammetry [38,39]. Considering the granular skeleton of the self-compacting concrete as a group of non-colloidal, rigid and polydisperse particles, the dynamic viscosity of the system can be estimated using Equation (1). The parameter ϕ_m , which depends on the shape and the size distribution of particles [19,22,23], acquires a theoretical value of about 0.648 in a monodisperse rigid spherical system of particles (regardless of its size). ϕ_m reaches a theoretical value of 0.744 in polydisperse systems, where the space between particles can be filled efficiently [14,22]. Experimental data adjusted with Equation (1) indicate that ϕ_m shows a decreasing trend with decreasing maximum particle size, which is related to decreased polydispersity of the particles [27]. The intrinsic

viscosity $[\eta]$ is a measure of the individual effect of particles on viscosity [19,22]. It is a parameter closely related to the characteristics of the aggregates [24–26], namely their shape, angularity and roughness [27], as well as their circularity [24,26]. $[\eta]$ is 2.5 for spherical and rigid particles [22], but when the particles deviate from this shape, $[\eta]$ reaches different values [19,24,25,40,41]. Besides, the intrinsic viscosity appears to increase with decreasing maximum particle size, the cause of this phenomenon being unknown [27], which is a new source of randomness.

In SCSFRC the interactions between particles due to shear [22] have to be considered, together with the overall sizes and shapes (the high concentration of aggregates, mainly, and steel fibers). In Equation (1) $[\eta]$ and ϕ_m depend on the shear rate, $\dot{\gamma}$, and the value of $[\eta]$ ϕ_m is approximately constant if the assumption of rigid spheres is applied to aggregates ($[\eta]$ $\phi_m \approx 1.9$ [22] or 2 [42,43]). The shear rate energy is also another source of randomness in the suspension, as it happens in systems formed only by cement paste.

The volume fractions and the geometric shape of the fibers (even if they are in equivalent proportions of diluted systems) are another component of uncertainty to the system, since fibers interact with the aggregates, giving place to variations in the behavior of the whole suspension. Fibers are considered as slender rigid solids whose translation and rotation are conditioned by the resistance of the self-compacting viscous concrete matrix. In the micromechanical models available in the scientific literature to predict the increase in dynamic viscosity produced by the addition of steel fiber into concrete, the fiber content is limited to a maximum volume fraction of 2% (to consider the diluted concentration hypothesis) and a maximum aspect ratio equal to 85 (to fulfill the rigid solid hypothesis) [15,22].

Finally, these considerations must be taken into account when using the constitutive equation that calculates the increase in dynamic viscosity of self-compacting concrete due to the inclusion of the fiber.

2.2. Description of the Bayesian Methodology

The use of Bayesian methodology is well known [44–46] and has been widely described in a previous work [21]. In short, Bayesian methods allow to combine the information of the expert knowledge (which is subjective), given by the prior distribution, and the information of the sample knowledge (which is the observation of reality), through Bayes' theorem, obtaining the posterior distribution (which is the combined one).

To apply the Bayesian methodology to a probabilistic model it is necessary to follow the next sequence [47]:

1. Choice of the likelihood family.
2. Choice of the prior distribution of the parameters:
 - By means of an imaginary sample (consulting an expert to provide a virtual sample representative of the prior knowledge).
 - Through previous non-updated information (consulting the expert).
 - Through our experimental data.
3. Obtaining data from the sample.
4. Calculation of the posterior distribution.
5. Through the combination of the posterior with the likelihood, the predictive distribution is obtained, which is the one we used.

Compared to frequentist statistics, Bayesian statistics have advantages such as obtaining better parameter estimations with small sample sizes, easy interpretation of the results when calculating the probabilities of the parameters, the introduction of measures of uncertainty, missing data and levels of variability [48].

2.3. Proposal of the Probabilistic Model and Bayesian Analysis of the Constitutive Model to Calculate the Dynamic Viscosity in SCSFRC

The purpose of this research is to convert the model to calculate the dynamic viscosity of SCSFRC into a parametric model using Bayesian analysis. The procedure considers

SCSFRC as a heterogeneous material composed of fibers in suspension in a more or less homogeneous granular fluid, which is the self-compacting matrix.

It is important to have good prior information, acquired using the experimental data or through expert consultation (i.e., scientific literature). It is very important to discern the quality of the information, especially if there is not enough data [47]. The Bayesian model to be created (its network) will consider the randomness of the dynamic viscosity mean value, and also the variability of the parameters. Proceeding this way, the parametric-deterministic model can be converted into a parametric-probabilistic model through the open-source software OpenBUGS [49]. This software incorporates a Bayesian inference program using the Markov Chain Monte Carlo method (MCMC) and the Gibbs Sampling methodology, a particular case of simulation algorithm of a Markov Chain. The software creates an acyclic graph with the hierarchical dependence structure of variables and parameters, and the posterior probability density functions of the parameters, together with the statistical values of the probabilistic model.

Self-Compacting Steel-Fiber Reinforced Concrete Suspensions

Self-compacting steel-fiber reinforced concrete can be considered as a multi-phase suspension composed of a heterogeneous phase (self-compacting concrete matrix) and steel fibers in suspension. Equation (1) includes the solid phases (powder, fine and coarse aggregate), and allows calculating the increase of the dynamic viscosity through Equation (2) [14]:

$$\eta^{\circ} = \left(1 - \frac{\phi_{fa}}{\phi_{mfa}}\right)^{-[\eta]_{fa} \phi_{mfa}} \left(1 - \frac{\phi_{FA}}{\phi_{mFA}}\right)^{-[\eta]_{FA} \phi_{mFA}} \left(1 - \frac{\phi_{CA}}{\phi_{mCA}}\right)^{-[\eta]_{CA} \phi_{mCA}} \quad (2)$$

where

$\eta^{\circ} = \frac{\eta_{SCC}}{\eta_p}$: Self-compacting concrete dimensionless viscosity.

η_{SCC} : Self-compacting concrete dynamic viscosity.

η_p : Cement paste dynamic viscosity.

ϕ_{fa} : Volume fraction of the powder phase.

ϕ_{mfa} : Particles' maximum packing fraction of the powder phase.

$[\eta]_{fa}$: Intrinsic viscosity taking into account the powder phase.

ϕ_{FA} : Volume fraction of the fine aggregate phase.

ϕ_{mFA} : Maximum packing fraction of the fine aggregate phase.

$[\eta]_{FA}$: Intrinsic viscosity of the fine aggregate phase.

ϕ_{CA} : Volume fraction of the coarse aggregate phase.

ϕ_{mCA} : Maximum packing fraction of the coarse aggregate phase.

$[\eta]_{CA}$: Intrinsic viscosity of the coarse aggregate phase.

In Equation (2), the parameters are treated as random variables which follow a probability density function of uniform type, within a range of maximum and minimum values. This uninformative priors have been chosen in order to let the data make the adequate corrections. These corrections can be seen in the posteriors when they separate from the uniform trend. We must note that when dependence exists, relatively small sizes are sufficient to produce large changes in the posteriors, which justifies the selected uninformative priors.

Equation (2) calculates the mean value of the dynamic viscosity of SCC, which is assumed to follow a normal probability density function, where the mean value is μ° , and the standard deviation value is σ . ϵ° is the residual value, which follows a normal family; moreover, ϵ° includes a uniform function of density.

The syntax of the extended model of the Krieger and Dougherty equation in a statistical format is:

$$\eta^\circ \sim N[\mu^\circ, \nu] \quad (3)$$

$$\mu^\circ = \left(1 - \frac{\phi_{fa}}{\phi_{mfa}}\right)^{-[\eta]_{fa} \phi_{mfa}} \left(1 - \frac{\phi_{FA}}{\phi_{mFA}}\right)^{-[\eta]_{FA} \phi_{mFA}} \left(1 - \frac{\phi_{CA}}{\phi_{mCA}}\right)^{-[\eta]_{CA} \phi_{mCA}} \quad (4)$$

$$\phi_{mfa} \sim U[\phi_{mfa \min}, \phi_{mfa \max}] \quad (5)$$

$$\phi_{mFA} \sim U[\phi_{mFA \min}, \phi_{mFA \max}] \quad (6)$$

$$\phi_{mCA} \sim U[\phi_{mCA \min}, \phi_{mCA \max}] \quad (7)$$

$$[\eta]_{fa} \sim U[[\eta]_{fa \min}, [\eta]_{fa \max}] \quad (8)$$

$$[\eta]_{FA} \sim U[[\eta]_{FA \min}, [\eta]_{FA \max}] \quad (9)$$

$$[\eta]_{CA} \sim U[[\eta]_{CA \min}, [\eta]_{CA \max}] \quad (10)$$

$$\sigma \sim U[\sigma_{\min}, \sigma_{\max}] \quad (11)$$

The incorporation of the steel fiber is taken into account by means of the model proposed by De La Rosa et al. (Equation (12)) to design self-compacting steel-fiber reinforced concrete [15]:

$$\eta_{SCSFRC} = \eta_p \left(1 - \frac{\phi_{fa}}{\phi_{mfa}}\right)^{-[\eta]_{fa} \phi_{mfa}} \left(1 - \frac{\phi_{FA}}{\phi_{mFA}}\right)^{-[\eta]_{FA} \phi_{mFA}} \left(1 - \frac{\phi_{CA}}{\phi_{mCA}}\right)^{-[\eta]_{CA} \phi_{mCA}} \left(1 + \frac{\phi_f}{\phi_\lambda}\right) \quad (12)$$

where

$$\phi_\lambda = \frac{3 \ln(2\lambda)}{\pi \lambda^2} \quad (13)$$

$$\eta_{SCSFRC} = \eta_{SCC} \left(1 + \frac{\phi_f}{\phi_\lambda}\right) \quad (14)$$

In Equation (13), λ is the aspect ratio of the steel fiber. It is obtained from the simplification of the model of Ghanbari et al. [22]. The only factor that can be parametrized is the number 3 which appears in both equations (the parameterization of this value will be carried out in Section 4).

Thus, the syntax of the model of De La Rosa et al. (Equation (12)) [15] in a statistical format is:

$$\eta^\circ \sim N[\mu^\circ, \nu] \quad (15)$$

$$\mu^\circ = \left(1 - \frac{\phi_{fa}}{\phi_{mfa}}\right)^{-[\eta]_{fa} \phi_{mfa}} \left(1 - \frac{\phi_{FA}}{\phi_{mFA}}\right)^{-[\eta]_{FA} \phi_{mFA}} \left(1 - \frac{\phi_{CA}}{\phi_{mCA}}\right)^{-[\eta]_{CA} \phi_{mCA}} \left(1 + \frac{\phi_f}{\phi_\lambda}\right) \quad (16)$$

and Equations (6) to (12).

3. Materials and Methods

A set of 56 self-compacting steel-fiber reinforced concretes (SCSFRCs) from [32] has been analyzed. The granular skeleton that SCSFRC is composed of rounded fine aggregate (0.125–4 mm) and rounded coarse aggregate (4–8 mm and 4–16 mm). The steel fibers are included in a ϕ_f range of 0.003 to 0.02, and their λ value is between 46.3 and 85.7. Rheological measurements of self-compacting steel-fiber reinforced concretes were done using a coaxial cylindrical viscometer (BML-Viscometer). The procedure to calculate the rheological parameters was the following: The rotation velocity of the outer cylinder of the viscometer was increased up to its maximum value and, once it was reached, the velocity was decreased [32].

In Ghanbari et al. [22], the dynamic viscosity of the cement pastes was calculated from data from the scientific literature on their composition [14,22,50,51] according to Ghanbari et al. [22]. In Tables 1 and 2, the composition of each base SCC, η_{SCC} , η_p , λ , ϕ_f and η_{SCSFRC} are included. The self-compacting steel-fiber reinforced concretes studied are derived from nine self-compacting matrices elaborated by Grünewald (Table 1) [32]. Table 2 shows the values of λ , ϕ_f , and η_{SCSFRC} of the combinations of concretes developed in [32].

In the Bayesian analysis, a total of 11,000 iterations in every model were done, through OpenBUGS, to obtain the samples of the variables (parameters of the deterministic models) that are considered as their density functions.

Table 1. Composition of base SCC [32] (w: Water; SP LR and HR: Superplasticizers; fa: Fly ash; FA: Fine aggregate, CA: Coarse aggregate).

Denomination	CEM I 52.5 R [kg/m ³]	CEM III 42.5 N [kg/m ³]	w [kg/m ³]	SP LR + SP HR [kg/m ³]	fa [kg/m ³]	FA [kg/m ³]	CA [kg/m ³]	η_{SCC} [Pa s]	η_p [Pa s]
OS1	249	155	172	2.58 + 1.58	142	913	682	69.2	0.404
OS2	263	149	181	2.88 + 1.44	173	876	655	59.4	0.413
OS3	249	149	171	2.59 + 2.12	146	1089	508	87.9	0.413
OS4	269	143	181	2.78 + 1.85	173	1045	487	56.0	0.413
OS5	0	335	155	2.10 + 1.26	168	1134	528	97.6	0.413
OS6	0	352	164	2.10 + 1.18	192	1089	508	81.0	0.422
OS7	0	367	173	2.17 + 1.09	217	1045	487	62.2	0.422
OS8	228	151	181	2.68 + 1.49	166	1100	467	71.3	0.395
OS9	246	164	188	2.73 + 1.31	180	1058	449	57.5	0.404

Table 2. λ , ϕ_f and η_{SCSFRC} of SCSFRC. Test set-up of measurements with BML–Viscometer [32].

Denomination	λ	ϕ_f	η_{SCSFRC} [Pa s]	Denomination	λ	ϕ_f	η_{SCSFRC} [Pa s]
OS1 80/30	78.5	0.008	167.8	OS5 80/30	78.5	0.005	195.8
OS1 80/60 BP	85.7	0.005	122.9	OS5 80/30	78.5	0.008	326.2
OS1 80/60 BP	85.7	0.008	125.0	OS5 80/60 BP	85.7	0.005	187.2
OS1 45/30	46.3	0.013	137.5	OS5 80/60 BP	85.7	0.008	261.8
OS1 80/30	78.5	0.005	116.8	OS5 45/30	46.3	0.013	245.3
OS1 45/30	46.3	0.010	109.9	OS5 45/30	46.3	0.015	280.3
OS2 80/30	78.5	0.008	171.1	OS6 80/30	78.5	0.008	266.8
OS2 80/30	78.5	0.010	223.2	OS6 80/30	78.5	0.010	344.2
OS2 80/60 BP	85.7	0.005	98.6	OS6 80/60 BP	85.7	0.005	182.8
OS2 80/60 BP	85.7	0.008	159.9	OS6 80/60 BP	85.7	0.008	301.8
OS2 45/30	46.3	0.018	262.0	OS6 45/30	46.3	0.015	211.5
OS2 45/30	46.3	0.015	144.3	OS6 45/30	46.3	0.018	265.0
OS3 80/30	78.5	0.005	143.1	OS7 80/30	78.5	0.008	209.1
OS3 80/30	78.5	0.008	199.3	OS7 80/30	78.5	0.010	306.1
OS3 80/60 BP	85.7	0.005	124.3	OS7 80/60 BP	85.7	0.008	224.8
OS3 80/60 BP	85.7	0.008	154.8	OS7 80/60 BP	85.7	0.010	233.1
OS3 45/30	46.3	0.015	237.0	OS7 65/40	64.9	0.013	206.1
OS3 45/30	46.3	0.018	279.3	OS7 45/30	46.3	0.015	157.1
OS4 80/30	78.5	0.010	245.3	OS7 45/30	46.3	0.018	204.4
OS4 80/60 BP	85.7	0.008	102.3	OS7 65/40	64.9	0.010	155.2
OS4 80/60 BP	85.7	0.010	199.7	OS8 80/30	78.5	0.003	80.8
OS4 45/30	46.3	0.018	145.7	OS8 80/30	78.5	0.005	141.4
OS4 65/40	64.9	0.015	221.1	OS8 65/20	64.3	0.005	98.8
OS4 80/30	78.5	0.008	156.5	OS8 65/20	64.3	0.008	210.1
OS4 45/30	46.3	0.015	117.5	OS9 80/30	78.5	0.005	92.2
OS4 45/30	46.3	0.020	176.1	OS9 80/30	78.5	0.008	162.4
OS4 65/40	64.9	0.013	182.2	OS9 65/20	64.3	0.005	120.7
				OS9 65/20	64.3	0.008	177.3
				OS9 65/20	64.3	0.010	142.6

The model analyzed is the one proposed by De La Rosa et al. to design SCSFRC [15], see Equation (12). Function ϕ_λ , Equation (13), depends on the π number and the aspect ratio of the steel fibers. Thus, the factor that can be parametrized is the number 3 ($=\delta$, i.e., the numerator of Equation (13)). It must be taken into account that the rest of the

parameters of the model (ϕ_{mj} , $[\eta]_f$), corresponding to Equation (2), also have been subjected to Bayesian analysis to find their density functions.

4. Results and Discussion

4.1. Bayesian Analysis Model in Self-Compacting Steel-Fiber Reinforced Concrete

Firstly, it has been analyzed if the δ parameter approaches 3. For this purpose, we use the experimental data of dynamic viscosity measured by Grünewald [32] in SCC, η_{SCC} and SCSFRC, η_{SCSFRC} . The model and the parameter definition domains for the Bayesian analysis, according to Equation (17), are:

$$\frac{\eta_{SCSFRC}}{\eta_{SCC}} = \left(1 + \frac{\phi_f}{\phi_\lambda}\right) \quad (17)$$

$$\eta^\diamond \sim N[\mu^\diamond, \nu] \quad (18)$$

$$\mu^\diamond = \left(1 + \frac{\pi \lambda^2 \phi_f}{\delta \ln(2\lambda)}\right) \quad (19)$$

$$\delta \sim U[0, 50] \quad (20)$$

$$\sigma \sim U[0, 400] \quad (21)$$

where

$\eta^\diamond = \frac{\eta_{SCSFRC}}{\eta_{SCC}}$: Non-dimensional viscosity of self-compacting steel-fiber reinforced concrete.

η_{SCSFRC} : Self-compacting steel-fiber concrete dimensionless viscosity.

η_{SCC} : Self-compacting concrete dynamic viscosity.

ϕ_f : Steel-fiber volume fraction.

λ : Steel-fiber aspect ratio.

δ : Parameter of the system when adding the steel fiber.

The upper value of the parameter δ ($\delta = 50$) is selected to obtain a wide range of calculations. Table 3 contains the statistics values of δ once the analysis of the model has been done. Figure 1 represents the non-parametric density functions of the parameter δ calculated with Equation (17) for different values of λ .

Table 3. Statistics of the parameter δ obtained for different aspect ratio values.

Aspect Ratio (λ)	Parameter	Mean	Std. Dev.	Percentage 2.5%	Median	Percentage 97.5%
46.3		14.350	1.819	11.570	14.100	18.640
64.3		16.950	6.000	9.954	15.170	34.610
64.9	δ	16.000	2.974	12.890	15.400	24.510
78.5		14.860	1.227	12.720	14.750	17.610
85.7		22.560	3.261	17.680	22.050	30.660

At this point, we have to keep in mind that the main objective is to evaluate the feasibility of Equation (12) [15] to design SCSFRC. The material of the powder phase used in the experimental investigation of Grünewald [32] is fly ash. Two uniform random variables for $[\eta]_{fa}$ are considered as priors in order to analyze the model. The first, $[\eta]_{fa} \sim U[4.30, 6.80]$, is obtained for cement pastes [21]. The second arises due to the sphericity of the fine particles of fly ash, which implies that the minimum value of $[\eta]_{fa}$ must be reduced from 4.30 to 2.50. Therefore, the widest range will be used in the analysis of the parameter $[\eta]_{fa}$, i.e., $[\eta]_{fa} \sim U[2.50, 6.80]$.

The parameters of Equations (15) and (16) of the model [15] in a statistical format are defined in the following values:

$$\phi_{mfa} \sim U [0.550, 0.830]$$

$$\phi_{mEA} \sim U [0.550, 0.717]$$

$$\phi_{mCA} \sim U [0.550, 0.894]$$

$$[\eta]_{fa} \sim U [2.5, 6.8]$$

$$[\eta]_{EA} \sim U [2.5, 9.0]$$

$$[\eta]_{CA} \sim U [2.5, 9.0]$$

$$\delta \sim U [0, 40]$$

$$\sigma \sim U [0, 400]$$

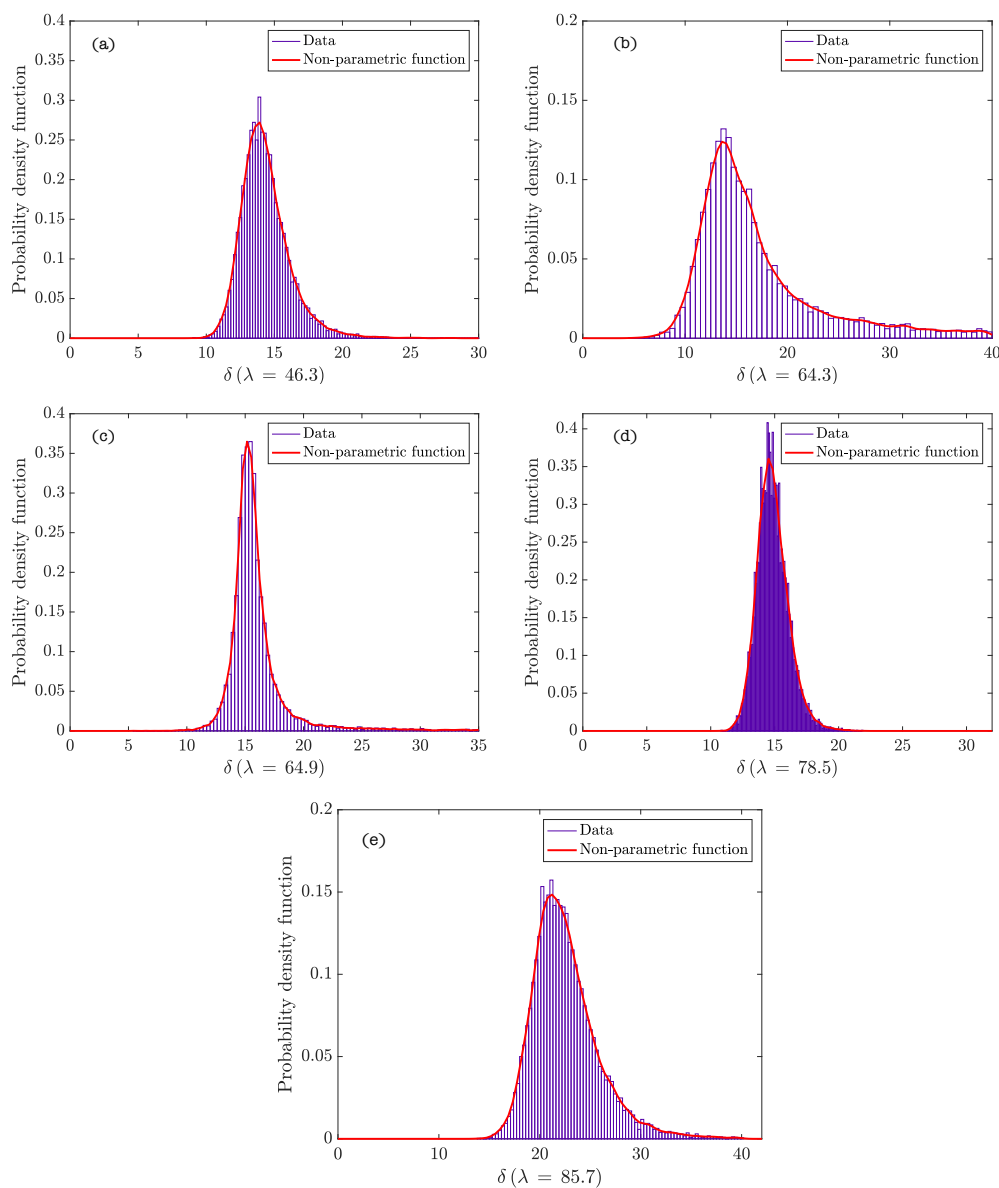


Figure 1. Probability density functions of δ for different values of λ ($\lambda = 46.3$ (a), 64.3 (b), 64.9 (c), 78.5 (d), and 85.7 (e)).

Figure 2 represents the hierarchy and dependence structure of the variables of the Bayesian network of the model. Five different SCSFRCs have been studied, corresponding

to five aspect ratios, ($\lambda = 46.3, 64.3, 64.9, 78.5,$ and 85.7). Table 4 includes the statistics values obtained after the Bayesian analysis. Figures 3 and 4 represent the probability density functions of the parameters for the phases of SCSFRC with $\lambda = 78.5$. The probability density function of the exponent of the Krieger and Dougherty equation ($\phi_{mi} [\eta]_i$) for the phases of SCSFRC is plotted in Figure 5. Finally, the bivariate histogram of the parameters ϕ_{mi} and $[\eta]_i$ of the phases for the SCSFRC with $\lambda = 78.5$ is shown in Figure 6.

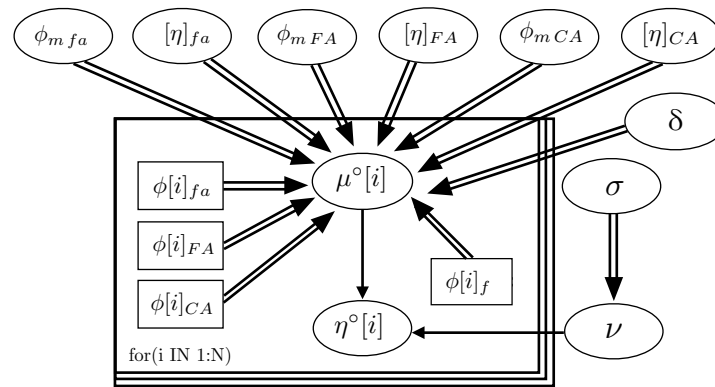


Figure 2. Bayesian network graph of the De La Rosa et al. model [15] for SCSFRC (from the investigation of Grünewald [32]).

Table 4. Statistics values of the parameters ϕ_{mi} , $[\eta]_i$, and δ_i for SCSFRC.

Aspect Ratio (λ)	Parameter	Mean	Std. Dev.	Percentage 2.5%	Median	Percentage 97.5%
46.3	ϕ_{mfa}	0.637	0.048	0.555	0.638	0.713
	$[\eta]_{fa}$	3.811	0.954	2.558	3.636	6.120
	ϕ_{mFA}	0.671	0.031	0.604	0.675	0.715
	$[\eta]_{FA}$	3.131	0.481	2.525	3.028	4.273
	ϕ_{mCA}	0.726	0.099	0.560	0.729	0.886
	$[\eta]_{CA}$	5.237	1.241	2.863	5.207	7.672
	δ	14.160	9.892	2.638	11.260	37.380
64.3	ϕ_{mfa}	0.633	0.048	0.554	0.633	0.713
	$[\eta]_{fa}$	4.603	1.221	2.612	4.572	6.680
	ϕ_{mFA}	0.663	0.036	0.586	0.669	0.715
	$[\eta]_{FA}$	3.306	0.507	2.545	3.258	4.409
	ϕ_{mCA}	0.723	0.099	0.559	0.722	0.885
	$[\eta]_{CA}$	5.424	1.785	2.649	5.338	8.723
	δ	20.110	10.290	4.039	19.350	38.730
64.9	ϕ_{mfa}	0.638	0.048	0.555	0.641	0.714
	$[\eta]_{fa}$	3.509	0.923	2.527	3.218	5.966
	ϕ_{mFA}	0.650	0.045	0.562	0.656	0.714
	$[\eta]_{FA}$	3.268	0.541	2.534	3.174	4.495
	ϕ_{mCA}	0.726	0.100	0.559	0.730	0.886
	$[\eta]_{CA}$	5.333	1.806	2.624	5.113	8.689
	δ	20.230	10.200	4.677	19.350	38.740
78.5	ϕ_{mfa}	0.633	0.048	0.554	0.633	0.713
	$[\eta]_{fa}$	5.007	0.810	3.419	4.987	6.531
	ϕ_{mFA}	0.697	0.017	0.657	0.701	0.716
	$[\eta]_{FA}$	2.706	0.195	2.506	2.652	3.223
	ϕ_{mCA}	0.736	0.096	0.563	0.742	0.887
	$[\eta]_{CA}$	3.407	0.696	2.533	3.261	5.104
	δ	5.184	2.765	2.318	4.357	12.440
85.7	ϕ_{mfa}	0.623	0.048	0.553	0.618	0.711
	$[\eta]_{fa}$	5.928	0.731	3.974	6.105	6.770
	ϕ_{mFA}	0.675	0.027	0.620	0.678	0.715
	$[\eta]_{FA}$	3.042	0.352	2.527	3.002	3.815
	ϕ_{mCA}	0.733	0.098	0.562	0.737	0.887
	$[\eta]_{CA}$	4.002	0.871	2.615	3.936	5.860
	δ	20.480	8.325	7.849	19.180	38.060

In this case, the Bayesian analysis of the SCSFRC was done with three phases of the Krieger and Dougherty equation (one powder phase plus two granular phases), and one steel-fiber phase to verify the model of De La Rosa et al. [15]. The powder phase shows similar values of ϕ_{mfa} for all the SCSFRC (≈ 0.63). However, the values of $[\eta]_{fa}$ are more dispersed. If we observe the non-parametric density functions (Figure 3a), ϕ_{mfa} shows a uniform density function in the same range of values, which is similar in the rest of the SCSFRCs not represented ($\lambda = 46.3, 64.3, 64.9,$ and 85.7). However, $[\eta]_{fa}$ (Figure 3b) shows a probability density function with a peak which grows as the aspect ratio of the fiber increases.

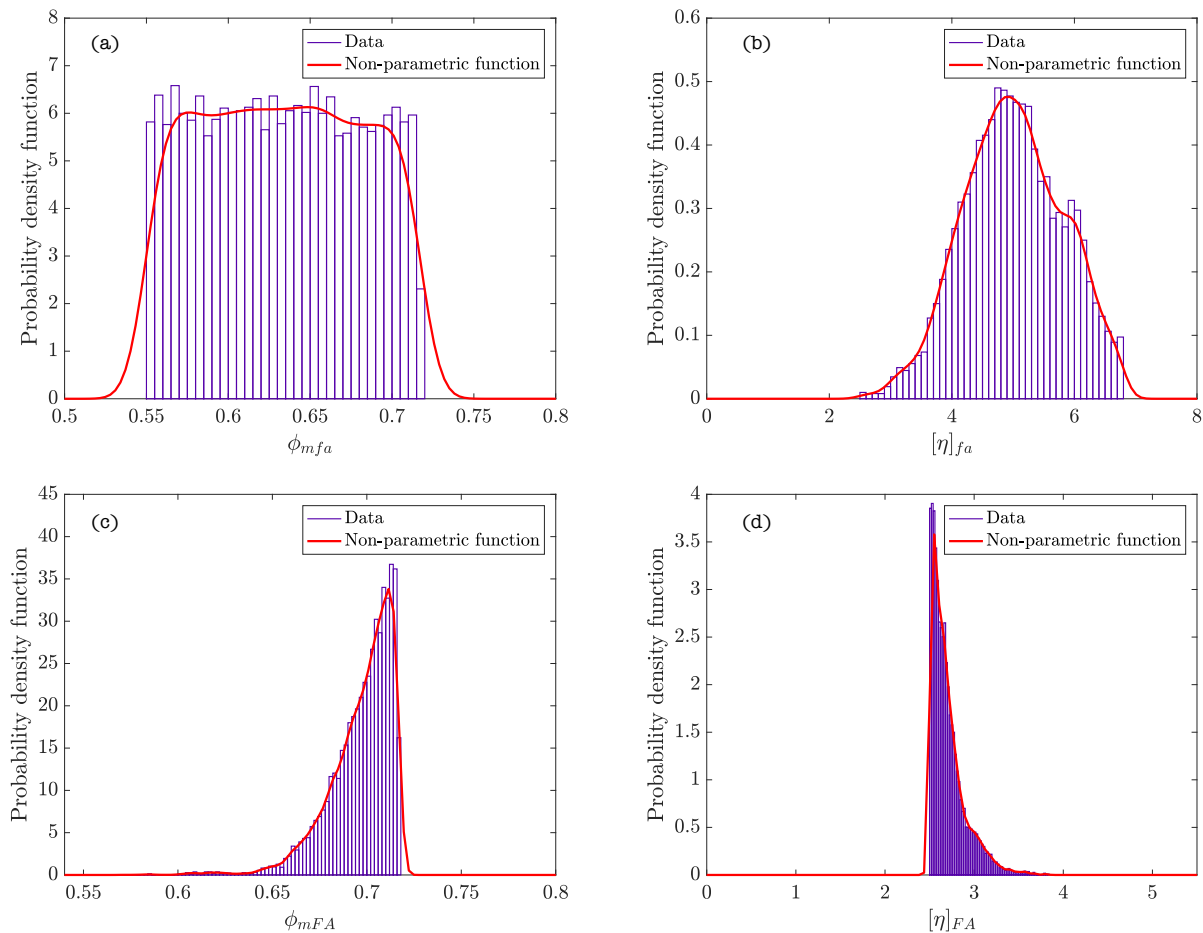


Figure 3. Probability density functions of ϕ_m and $[\eta]$ for the powder phase ((a,b), respectively), and fine granular phase ((c,d), respectively) in SCSFRC ($\lambda = 78.5$).

Regarding ϕ_{mFA} , the mean value is roughly 0.67; the same conclusion can be obtained with $[\eta]_{FA}$ (≈ 3.0). Both non-parametric density functions (Figure 3c) show the same trend probability peaks about the same values in every SCSFRC.

The mean values obtained for ϕ_{mCA} are 0.73 regardless of the specific type of SCSFRC. The mean values calculated for $[\eta]_{CA}$ are approximately 5.0 except for those SCSFRC with a higher aspect ratio of the fiber, which figures lower than 5.0. The non-parametric density functions are approximately uniform for ϕ_{mCA} (Figure 4a) in every SCSFRC. As to $[\eta]_{CA}$, the density function shows a peak of different values depending on λ : The lower the aspect ratio, the higher the value $[\eta]_{CA}$ with a maximum probability (Figure 4b).

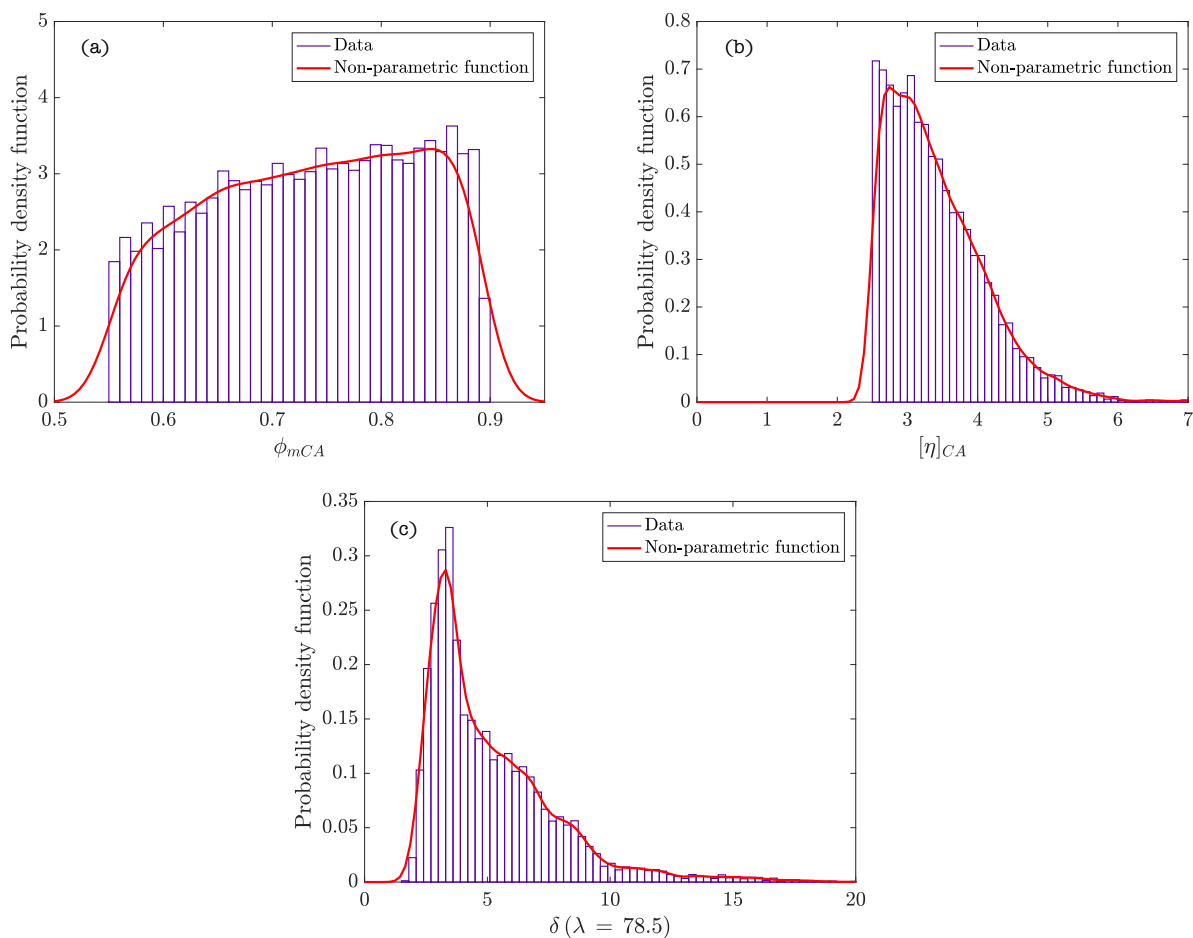


Figure 4. Probability density functions of ϕ_m and $[\eta]$ for the coarse granular phase ((a,b), respectively) and δ parameter (c) in SCSFRC ($\lambda = 78.5$).

Comparing these results with those obtained for the analysis of SCC with respect to the granular phases (fine and coarse aggregate), we realize that the values of the parameters are very similar. This fact means that the Bayesian analysis in two and three phases for the SCC offers approximately the same results and conclusions.

According to the results of the Bayesian analysis (Table 4), it is verified that the parameter δ can acquire values much higher than 3, except for the fiber with $\lambda = 78.5$ ($\delta \approx 5$). This trend is the same as that previously observed while fixing the ranges of δ (Table 3). In Figure 4c we can observe the non-parametric density function of δ for a steel fiber with $\lambda = 78.5$, which reaches a clear peak of probability. For the rest of the λ values, this peak is not so clear, and the density functions are smoother but reach much higher values than those for $\lambda = 78.5$. Probably, this is because Equation (13) is an approximation of the contribution of the fiber in the effective stress tensor obtained by following the procedure of Phan–Thien and Karihaloo [29], who derive the effective stress tensor, and the fiber contributed stress from the slender body theory of Russel [29,52].

Figure 5 shows that the most probable value for the exponent of the Krieger and Dougherty equation is different from the theoretical value of 1.9. This is true in all phases except for the fine aggregate phase. The extension of the probability density function of the powder and coarse aggregate phases represents the range that the exponent could acquire. Finally, the bivariate histogram of the parameters ϕ_{m_i} and $[\eta]_i$ of the phases of SCSFRC ($\lambda = 78.5$) is represented in Figure 6.

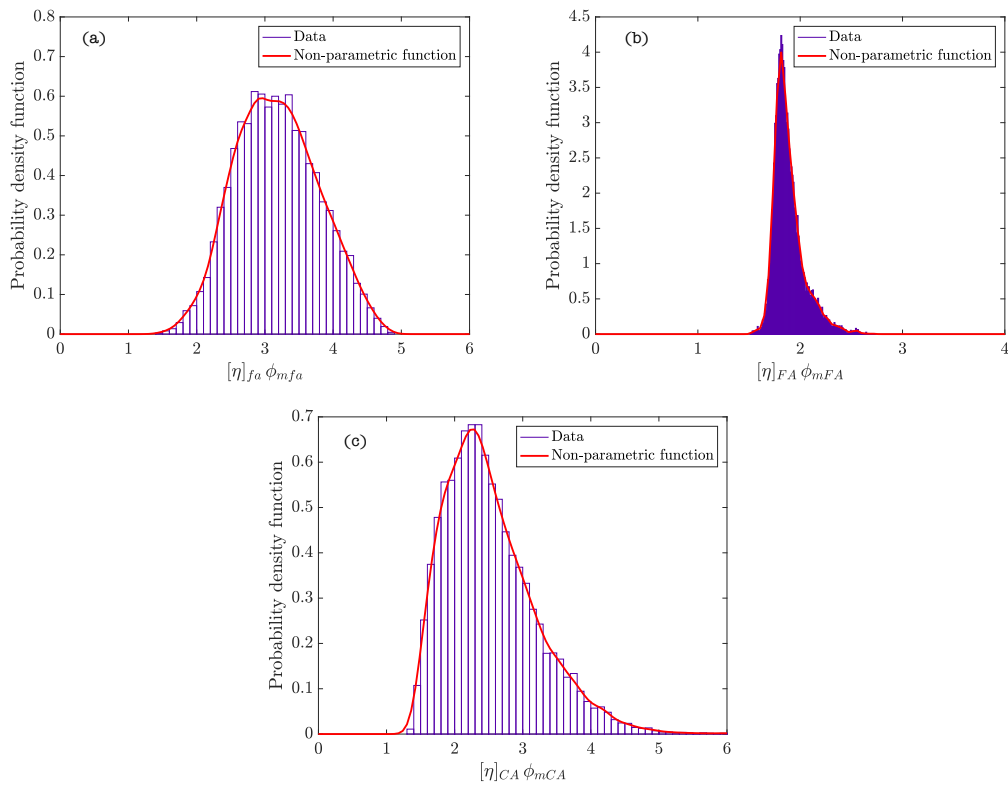


Figure 5. Probability density functions of $\phi_{mi} [\eta]_i$; ((a) powder phase; (b) fine granular phase; (c) coarse granular phase) in SCSFRC ($\lambda = 78.5$).

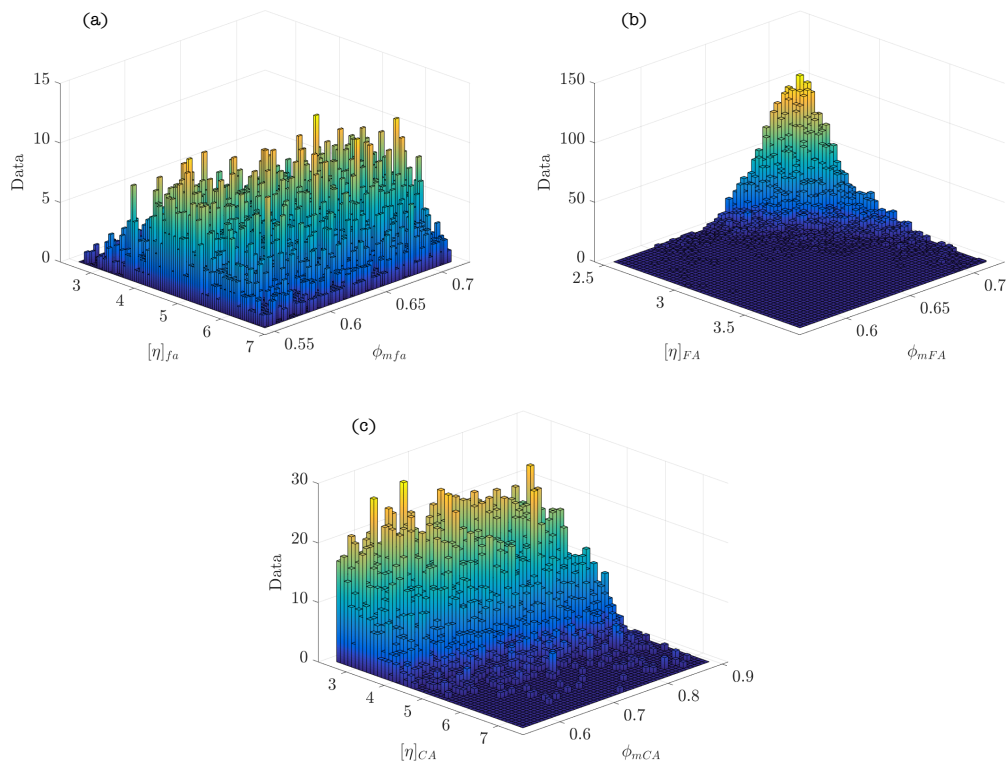


Figure 6. Bivariate histogram of ϕ_{mi} and $[\eta]_i$; ((a) powder phase; (b) fine granular phase; (c) coarse granular phase) composing SCSFRC ($\lambda = 78.5$).

4.2. Application of the Bayesian Analysis Results to the Experimental Data

The same process used for self-compacting mortar and self-compacting concrete [21] was followed for SCSFRC. For this, the mean values of the parameters obtained in the Bayesian analysis of the model to the data of Grünewald (Tables 5 and 6) [32] were applied. After, the results obtained were compared with those calculated using the values of Abo-Daheer et al. ($\phi_{m\,fa} = 0.524$ for powder phase; $\phi_{m\,FA} = 0.63$ for powder and fine aggregate phase; $\phi_{m\,CA} = 0.74$ for powder, fine and coarse aggregate phases; $\phi_{m,i} [\eta]_i = 1.9$) [14] and Ghanbari et al. ($\delta = 3$) [22].

Table 5. Experimental values, models' values and estimated error for SCSFRC (Grünewald [32]: Series OS1–OS4).

Denomination	Experimental η_{SCSFRC} [Pa s]	Bayesian Calculus Equation (17), η_{SCSFRC} [Pa s]	Bayesian Calculus Equation (12), η_{SCSFRC} [Pa s]	Theoretical Calculus [14,22], η_{SCSFRC} [Pa s]	Error with Bayesian Calculus Equation (17) [%]	Error with Bayesian Calculus Equation (12) [%]	Error with Theoretical Calculus [14,22] [%]
OS1 80/30	167.8	205.5	161.7	270.8	22.5	3.6	61.4
OS1 80/60 BP	122.9	139.3	108.8	217.1	13.4	11.5	76.6
OS1 80/60 BP	125.0	174.4	137.5	313.0	39.5	10.0	150.4
OS1 45/30	137.5	160.6	132.2	184.0	16.8	3.8	33.8
OS1 80/30	116.8	160.1	115.9	189.0	37.0	0.8	61.8
OS1 45/30	109.9	142.3	117.1	152.3	29.5	6.5	38.6
OS2 80/30	171.1	176.4	139.4	206.8	3.1	18.6	20.8
OS2 80/30	223.2	215.4	178.8	269.3	3.5	19.9	20.6
OS2 80/60 BP	98.6	119.6	91.3	165.7	21.3	7.4	68.1
OS2 80/60 BP	159.9	149.7	115.4	239.0	6.4	27.8	49.4
OS2 45/30	262.0	169.2	122.9	189.0	35.4	53.1	27.9
OS2 45/30	144.3	153.5	111.5	164.7	6.4	22.8	14.2
OS3 80/30	143.1	203.3	133.8	306.6	42.1	6.5	114.2
OS3 80/30	199.3	261.0	186.7	439.4	31.0	6.3	120.5
OS3 80/60 BP	124.3	177.0	132.4	352.2	42.4	6.6	183.3
OS3 80/60 BP	154.8	221.5	167.4	507.8	43.1	8.1	228.1
OS3 45/30	237.0	227.2	160.0	350.1	4.2	32.5	47.7
OS3 45/30	279.3	250.4	176.5	401.7	10.4	36.8	43.8
OS4 80/30	245.3	203.3	190.4	373.6	17.2	22.4	52.3
OS4 80/60 BP	102.3	141.1	126.2	331.5	37.9	23.3	224.1
OS4 80/60 BP	199.7	169.5	152.5	433.1	15.1	23.6	116.9
OS4 45/30	145.7	159.5	121.8	262.2	9.5	16.4	80.0
OS4 65/40	221.1	201.5	159.2	396.1	8.9	28.0	79.2
OS4 80/30	156.5	166.3	148.4	286.9	6.3	5.2	83.3
OS4 45/30	117.5	144.7	110.4	228.6	23.2	6.0	94.5
OS4 45/30	176.1	174.3	133.1	295.9	1.0	24.4	68.0
OS4 65/40	182.4	177.2	141.3	334.6	2.8	22.5	83.4

Table 6. Experimental values, models' values, and estimated error for SCSFRC (Grünewald [32]): Series OS5–OS9).

Denomination	Experimental η_{SCSFRC} [Pa s]	Bayesian Calculus Equation (17), η_{SCSFRC} [Pa s]	Bayesian Calculus Equation (12), η_{SCSFRC} [Pa s]	Theoretical Calculus [14,22], η_{SCSFRC} [Pa s]	Error with Bayesian Calculus Equation (17) [%]	Error with Bayesian Calculus Equation (12) [%]	Error with Theoretical Calculus [14,22] [%]
OS5 80/30	195.8	225.7	236.3	373.6	15.3	20.7	241.0
OS5 80/30	326.2	289.8	329.7	331.5	11.2	1.1	193.4
OS5 80/60 BP	187.2	196.5	273.3	433.1	5.0	46.0	309.8
OS5 80/60 BP	261.8	245.9	345.4	262.2	6.1	31.9	322.5
OS5 45/30	245.3	226.5	271.6	396.1	7.7	10.7	165.1
OS5 45/30	280.3	252.2	302.6	396.1	10.0	8.0	172.1
OS6 80/30	266.8	240.5	242.5	525.9	9.9	9.1	97.1
OS6 80/30	344.2	293.7	311.2	684.9	14.7	9.6	99.0
OS6 80/60 BP	182.8	163.1	185.4	421.5	10.8	1.4	130.6
OS6 80/60 BP	301.8	204.1	234.3	607.8	32.4	22.4	101.4
OS6 45/30	211.5	209.3	188.6	419.0	1.0	10.8	98.1
OS6 45/30	265.0	230.7	208.0	480.7	12.9	21.5	81.4
OS7 80/30	209.1	184.7	195.8	353.4	11.7	6.4	69.0
OS7 80/30	306.1	225.5	251.2	460.2	26.3	17.9	50.3
OS7 80/60 BP	224.8	156.7	179.0	408.4	30.3	20.4	81.7
OS7 80/60 BP	233.1	188.2	216.3	533.6	19.2	7.2	128.9
OS7 65/40	206.1	196.9	166.9	412.1	4.5	19.0	100.0
OS7 45/30	157.1	160.7	133.3	281.6	2.3	15.1	79.2
OS7 45/30	204.4	177.2	147.0	323.0	13.3	28.1	58.0
OS7 65/40	155.2	169.9	145.8	336.3	9.5	6.0	116.7
OS8 80/30	80.8	118.1	67.8	138.4	46.2	16.1	71.3
OS8 80/30	141.4	164.9	112.1	244.3	16.6	20.7	72.7
OS8 65/20	98.8	128.6	124.2	180.4	30.2	25.7	82.6
OS8 65/20	210.1	157.3	149.3	254.3	25.1	28.9	21.0
OS9 80/30	92.2	133.0	93.0	174.6	44.2	0.9	89.3
OS9 80/30	162.4	170.7	129.7	250.2	5.1	20.1	54.1
OS9 65/20	120.7	103.7	90.5	128.9	14.1	25.0	6.8
OS9 65/20	177.3	126.8	108.8	181.7	28.5	38.6	2.5
OS9 65/20	142.6	150.0	127.1	234.6	5.2	10.9	64.5

If we set an error of $\leq 25\%$ between the experimental rheological measurements of Grünewald [32], and the estimation made with the mean of the parameters calculated with the Bayesian method, we obtain an excellent approximation of 80% of the global data. However, if we set the typical parameters used in the Krieger and Dougherty

model proposed by Abo-Daheer et al. [14] for the terms of the model of De La Rosa et al. (Equation (12)) [15], and the parameter proposed by Ghanbari et al. [22] for the inclusion of steel fiber in the mentioned model [15], we obtain an approximation of 11% of the global data. Indeed, we obtain a good approximation of 70% of the global data if we use the simplest model (Equation (17)).

5. Conclusions

This article extends the research on the transformation of deterministic models into probabilistic models for the study of the dynamic viscosity in cementitious suspensions, in this case applying the methodology to self-compacting steel fiber reinforced concrete (SCSFRC). If the uncertainty associated with the nature, geometry and particle size distribution of cementitious suspensions already required considering the Krieger and Dougherty equation with random variables (in terms of its parameters), the inclusion of steel fibers in the system also advises using the Bayesian approach.

The Bayesian analysis was applied to a deterministic micromechanical model, which calculates the dynamic viscosity of SCSFRC, to obtain the samples of the variables as probability functions (density or distribution), which are the parameters of the deterministic models. Through the open-source software OpenBUGS, which employs Markov Chain Monte Carlo and Gibbs Sampling methods, the simulations were performed. An acyclic graph describes the hierarchy and independence of variables and conditions the probability density function of the parameters of the micromechanical model. The analysis attributes the calculated distributions to all the causes that physically condition them, not just to a single cause. The main results reached in this article are:

- The Bayesian methodology responds to questions in complex systems (fluid paste, aggregates and rigid fibers) with complex models (Krieger and Dougherty equation and De La Rosa et al. equation) about the probability of any parameter of those to reach a specific value in the function of the type of material employed.
- This change of paradigm about the use of probabilistic models in this type of systems can be useful for cementitious material designers, as well as for other engineering models.
- When the values of the parameters calculated through the Bayesian analysis are applied in the model, the approximation to the experimentally measured values of dynamic viscosity in SCSFRC is better than the theoretical values suggested by the scientific literature (calculations using the Bayesian mean values were better than those made with the theoretical values, considerably decreasing the error).

These results indicate the usefulness of Bayesian analysis in obtaining better estimates of the models used in engineering and science.

Author Contributions: Conceptualization, Á.D.L.R. and E.C.; methodology, all authors; simulations, Á.D.L.R.; validation, Á.D.L.R. and G.R.; resources: G.R. and R.M.; writing—original draft preparation, Á.D.L.R.; writing—review and editing, all authors; supervision, G.R.; funding acquisition, G.R. All authors have read and agreed to the published version of the manuscript.

Funding: The authors acknowledge the funding obtained through the *Ministerio de Innovación, Ciencia y Universidades*, Spain, through PID2019-110928RB-C31 and RTC-2017-6736-3 projects, and from *Junta de Comunidades de Castilla-La Mancha* through SBPLY/19/180501/000220 research project, Spain.

Institutional Review Board Statement: Not applicable.

Informed Consent Statement: Not applicable.

Data Availability Statement: Not applicable.

Conflicts of Interest: The authors declare no conflict of interest.

Abbreviations

SCC	Self-compacting concrete
SCSFRC	Self-compacting steel-fiber reinforced concrete
i	Number of nodes
j	Number of phase of SCC
n	Number of conditional probability density functions
N	Normal probability density function
U	Uniform probability density function
ε°	Residual error for non-dimensional dynamic viscosity of SCC
δ	Parameter of the system when adding the steel fiber
η	Dynamic viscosity
η_{SCC}	Dynamic viscosity of SCC
η_p	Cement paste dynamic viscosity
η_0	Fluid phase dynamic viscosity
η°	Non-dimensional dynamic viscosity of SCC
η^\diamond	$= \frac{\eta_{SCSFRC}}{\eta_{SCC}}$: non-dimensional viscosity of SCSFRC
$[\eta]$	Intrinsic viscosity
$[\eta]_{CA}$	Intrinsic viscosity of the coarse aggregate phase in SCC
$[\eta]_{fa}$	Intrinsic viscosity of the powder phase in SCC
$[\eta]_{FA}$	Intrinsic viscosity of the fine aggregate phase in SCC
λ	Aspect ratio of steel fiber
μ°	Mean value for non-dimensional dynamic viscosity of SCC
μ^\diamond	Mean value for non-dimensional dynamic viscosity of SCSFRC
$v = \frac{1}{\sigma^2}$	Auxiliar variable for the model of probability
π_i	Set of nodes X_i in \mathcal{G}
σ	Standard deviation of the sample
ϕ_f	Volume fraction of steel fiber
ϕ_{CA}	Coarse aggregate volume fraction
ϕ_{fa}	Powder volume fraction
ϕ_{FA}	Fine aggregate volume fraction
ϕ_m	Maximum packing density of particles
ϕ_{mCA}	Maximum packing density of particles in the coarse aggregate phase in SCSFRC
ϕ_{mfa}	Maximum packing density of particles in the powder phase in SCSFRC
ϕ_{mFA}	Maximum packing density of particles in the fine aggregate phase in SCSFRC
ϕ_λ	Function which depends on the π number and the aspect ratio of the steel fiber

References

1. Feys, D.; Cepuritis, R.; Jacobsen, S.; Lesage, K.; Secrieru, E.; Yahia, A. Measuring rheological properties of cement pastes: Most common techniques, procedures and challenges. *RILEM Tech. Lett.* **2017**, *2*, 129–135. [\[CrossRef\]](#)
2. Ferrara, L. High performance fibre reinforced cementitious composites: Six memos for the XXI century societal and economical challenges of civil engineering. *Case Stud. Constr. Mater.* **2019**, *10*, e00219. [\[CrossRef\]](#)
3. Menna, C.; Mata-Falcón, J.; Bos, F.; Vantghem, G.; Ferrara, L.; Asprone, D.; Salet, T.; Kaufmann, W. Opportunities and challenges for structural engineering of digitally fabricated concrete. *Cem. Concr. Res.* **2020**, *133*, 106079. [\[CrossRef\]](#)
4. Roussel, N. Rheological requirements for printable concretes. *Cem. Concr. Res.* **2018**, *112*, 76–85. [\[CrossRef\]](#)
5. Jeong, H.; Han, S.; Choi, S.; Lee, Y.; Yi, S.; Kim, K. Rheological property criteria for buildable 3D printing concrete. *Materials* **2019**, *12*, 657. [\[CrossRef\]](#) [\[PubMed\]](#)
6. Feys, D.; Khayat, K.; Pérez-Schell, A.; Khatib, R. Prediction of pumping pressure by means of new tribometer for highly-workable concrete. *Cem. Concr. Compos.* **2015**, *57*, 102–115. [\[CrossRef\]](#)
7. Ivanova, I.; Mechtcherine, V. Effects of volume fraction and surface area of aggregates on the static yield stress and structural build-up of fresh concrete. *Materials* **2020**, *13*, 1551. [\[CrossRef\]](#)
8. Fataei, S.; Secrieru, E.; Mechtcherine, V. Experimental insights into concrete flow-regimes subject to shear-induced particle migration (SIPM) during pumping. *Materials* **2020**, *13*, 1233. [\[CrossRef\]](#)
9. Wangler, T.; Lloret, E.; Reiter, L.; Hack, N.; Gramazio, F.; Kohler, M.; Bernhard, M.; Dillenburger, B.; Buchli, J.; Roussel, N.; et al. Digital concrete: Opportunities and challenges. *RILEM Tech. Lett.* **2016**, *1*, 67–75. [\[CrossRef\]](#)
10. Wangler, T.; Roussel, N.; Bos, F.; Salet, A.; Flatt, R. Digital concrete: A review. *Cem. Concr. Res.* **2019**, *123*, 105780. [\[CrossRef\]](#)
11. Roussel, N.; Gram, A.; Cremonesi, M.; Ferrara, L.; Krenzer, K.; Mechtcherine, V.; Shyshko, S.; Skocec, J.; Spangenberg, J.; Svec, O.; et al. Numerical simulations of concrete flow: A benchmark comparison. *Cem. Concr. Res.* **2016**, *79*, 265–271. [\[CrossRef\]](#)

12. Wallevik, J.; Wallevik, O. Analysis of shear rate inside a concrete truck mixer. *Cem. Concr. Res.* **2017**, *95*, 9–17. [[CrossRef](#)]
13. Reinold, J.; Naidu Nerella, V.; Mechtcherine, V.; Meschke, G. Extrusion process simulation and layer shape prediction during 3D-concrete-printing using the particle finite element method. *Autom. Constr.* **2022**, *136*, 104173. [[CrossRef](#)]
14. Abo Dhaheer, M.; Al-Rubaye, M.; Alyhya, W.; Karihaloo, B.; Kulasegaram, S. Proportioning of self-compacting concrete mixes based on target plastic viscosity and compressive strength: Part I—Mix design procedure. *J. Sustain. Cem.-Based Mater.* **2016**, *5*, 199–216. [[CrossRef](#)]
15. De La Rosa, Á.; Poveda, E.; Ruiz, G.; Cifuentes, H. Proportioning of self-compacting steel-fiber reinforced concrete mixes based on target plastic viscosity and compressive strength: Mix-design procedure and experimental validation. *Constr. Build. Mater.* **2018**, *189*, 409–419. [[CrossRef](#)]
16. Ferrara, L.; Park, Y.; Shah, S. A method for mix-design of fiber-reinforced self-compacting concrete. *Cem. Concr. Res.* **2007**, *37*, 957–971. [[CrossRef](#)]
17. Deeb, R.; Ghanbari, A.; Karihaloo, B. Development of self-compacting high and ultra high performance concretes with and without steel fibres. *Cem. Concr. Compos.* **2012**, *34*, 185–190. [[CrossRef](#)]
18. Krieger, I.; Dougherty, T. A mechanism for non-Newtonian flow in suspensions of rigid spheres. *J. Rheol.* **1959**, *3*, 137–152. [[CrossRef](#)]
19. Struble, L.; Sun, G. Viscosity of portland cement pastes as a function of concentration. *Adv. Cem. Based Mater.* **1995**, *2*, 62–69. [[CrossRef](#)]
20. De La Rosa, Á.; Poveda, E.; Ruiz, G.; Moreno, R.; Cifuentes, H.; Garijo, L. Determination of the plastic viscosity of superplasticized cement pastes through capillary viscometers. *Constr. Build. Mater.* **2020**, *260*, 119715. [[CrossRef](#)]
21. De La Rosa, Á.; Ruiz, G.; Castillo, E.; Moreno, R. Calculation of dynamic viscosity in concentrated cementitious suspensions: Probabilistic approximation and Bayesian analysis. *Materials* **2021**, *14*, 1971. [[CrossRef](#)]
22. Ghanbari, A.; Karihaloo, B.L. Prediction of the plastic viscosity of self-compacting steel fibre reinforced concrete. *Cem. Concr. Res.* **2009**, *39*, 1209–1216. [[CrossRef](#)]
23. Burgos-Montes, O.; Alonso, M.; Puertas, F. Viscosity and water demand of limestone and fly ash-blended cement pastes in the presence of superplasticisers. *Constr. Build. Mater.* **2013**, *48*, 417–423. [[CrossRef](#)]
24. Choi, M. Numerical prediction on the effects of the coarse aggregate size to the pipe flow of pumped concrete. *J. Adv. Concr. Technol.* **2014**, *12*, 239–249. [[CrossRef](#)]
25. Barnes, H.; Hutton, J.; Walters, K. *An Introduction to Rheology*, 3rd ed.; Elsevier: Amsterdam, The Netherlands, 1993; pp. 119–128.
26. Szecsy, R. Concrete Rheology. Ph.D. Thesis, University of Illinois at Urbana, Urbana, IL, USA, 1997.
27. Salinas, A.; Feys, D. Estimation of lubrication layer thickness and composition through reverse engineering of interface rheometry tests. *Materials* **2020**, *13*, 1799. [[CrossRef](#)] [[PubMed](#)]
28. Batchelor, G. The stress generated in a non-dilute suspension of elongated particles by pure straining motion. *J. Fluid Mech. Digit. Arch.* **1971**, *46*, 813–829. [[CrossRef](#)]
29. Phan-Thien, N.; Karihaloo, B. Materials with negative Poisson ratio: A qualitative microstructural model. *J. Appl. Mech.* **1994**, *61*, 1001–1004. [[CrossRef](#)]
30. Muñoz-Calvente, M.; Castillo, E.; Fernández-Canteli, A.; Blasón, S.; Álvarez, A. Los percentiles de los percentiles: Un paso más allá en fatiga. *An. Mec. Fract.* **2019**, *36*, 444–449.
31. Gómez-Rubio, V. *Bayesian Inference with INLA*, Chapman and Hall-CRC ed.; CRC Press: Boca Raton, FL, USA, 2020.
32. Grünwald, S. Performance-Based Design of Self-Compacting Fibre Reinforced Concrete. Ph.D. Thesis, Technische Universiteit Darmstadt, Delft, The Netherlands, 2004.
33. Castillo, E.; Gutiérrez, J.; Hadi, A. *Expert Systems and Probabilistic Network Models*; Springer: New York, NY, USA, 1997.
34. Moreno, R. *Reología de Suspensiones Cerámicas*; Consejo Superior de Investigaciones Científicas: Madrid, Spain, 2005.
35. Berrezueta, E.; Cuervas-Mons, J.; Rodríguez-Rey, Á.; Ordóñez-Casado, B. Representativity of 2D Shape Parameters for Mineral Particles in Quantitative Petrography. *Minerals* **2019**, *9*, 768. [[CrossRef](#)]
36. Santamarina, J.; Cho, G. Soil Behavior: The Role of Particle Shape. In Proceedings of the Advances in Geotechnical Engineering: The Skempton Conference, London, UK, 29–31 March 2004.
37. Ren, Q.; Ding, L.; Dai, X.; Jiang, Z.; Ye, G.; De Schutter, G. Determination of specific surface area of irregular aggregate by random sectioning and its comparison with conventional methods. *Constr. Build. Mater.* **2021**, *273*, 122019. [[CrossRef](#)]
38. Isik Ozturk, H.; Rashidzade, I. A photogrammetry based method for determination of 3D morphological indices of coarse aggregates. *Constr. Build. Mater.* **2020**, *262*, 120794. [[CrossRef](#)]
39. Paxão, A.; Resende, R.; Fortunato, E. Photogrammetry for digital reconstruction of railway ballast particles—A cost-efficient method. *Constr. Build. Mater.* **2018**, *191*, 963–976. [[CrossRef](#)]
40. Pabst, W.; Gregorova, E.; Berthold, C. Particle shape and suspension rheology of short-fiber systems. *J. Eur. Ceram. Soc.* **2006**, *26*, 149–160. [[CrossRef](#)]
41. Brenner, H. Rheology of a dilute suspension of axisymmetric Brownian particles. *Int. J. Multiph. Flow* **1974**, *1*, 195–341. [[CrossRef](#)]
42. Maron, S.; Pierce, P. Application of ree-eyring generalized flow theory to suspensions of spherical particle. *J. Colloids Sci.* **1956**, *11*, 80–95. [[CrossRef](#)]
43. Shewan, H.; Stokes, J. Analytically predicting the viscosity of hard sphere suspensions from the particle size distribution. *J. Non-Newton. Fluid Mech.* **2015**, *222*, 72–81. [[CrossRef](#)]

44. Castillo, E.; Menéndez, J.; Sánchez-Cambronero, S. Predicting traffic flow using Bayesian networks. *Transp. Res. Part B* **2008**, *42*, 482–509. [[CrossRef](#)]
45. Castillo, E.; Gutiérrez, J. *Sistemas Expertos y Modelos de Redes Probabilísticas*; Academia de Ingeniería, D.L.: Madrid, Spain, 1997.
46. Cowles, M. *Applied Bayesian Statistics with R and OpenBUGS Examples*; Springer: New York, NY, USA, 2013.
47. Castillo, E.; Menéndez, J.; Sánchez-Cambronero, S.; Calviño, A.; Sarabia, J. A hierarchical optimization problem: Estimating traffic flow using Gamma random variables in a Bayesian context. *Comput. Oper. Res.* **2014**, *41*, 240–251. [[CrossRef](#)]
48. Ruiz-Benito, P.; Andivia, E.; Archambeau, J.; Astigarraga, J.; Barrientos, R.; Cruz-Alonso, V.; Florencio, M.; Gómez, D.; Martínez-Baroja, L.; Quiles, P.; et al. Ventajas de la estadística Bayesiana frente a la frecuentista: ¿Por qué nos resistimos a usarla? *Ecosistemas* **2018**, *27*, 136–139. [[CrossRef](#)]
49. OpenBUGS. 2009. Available online: www.openbugs.net (accessed on 10 October 2021).
50. Sun, Z.; Voigt, T.; Shah, S. Rheometric and ultrasonic investigations of viscoelastic properties of fresh portland cement pastes. *Cem. Concr. Res.* **2006**, *36*, 278–287. [[CrossRef](#)]
51. Nehdi, M.; Rahman, M. Estimating rheological properties of cement pastes using various rheological models for different test geometry, gap and surface friction. *Cem. Concr. Res.* **2004**, *34*, 1993–2007. [[CrossRef](#)]
52. Russel, W. On the effective moduli of composite materials: Effect of fiber length and geometry at dilute concentrations. *Z. für Angew. Mathematik Phys.* **1973**, *23*, 434–464. [[CrossRef](#)]